Trypanosoma cruzi glycosomal glyceraldehyde-3-phosphate dehydrogenase: structure, catalytic mechanism and targeted inhibitor design

D.H.F. Souza[a], R.C. Garratt[a], A.P.U. Araújo[a], B.G. Guimarães[a], W.D.P. Jesus[a], P.A.M. Michels[b], V. Hannaert[b], G. Oliva[a,*]

[a] *Instituto de Física de São Carlos, USP, P.O. Box 369, 13560-970 São Carlos, SP, Brazil*
[b] *Research Unit for Tropical Diseases, Christian de Duve Institute of Cellular Pathology (ICP) and Catholic University of Louvain, Ave. Hippocrate 74, B-1200 Brussels, Belgium*

Received 7 January 1998; revised version received 5 February 1998

Abstract The structure of the enzyme glyceraldehyde-3-phosphate dehydrogenase (GAPDH) from glycosomes of the parasite *Trypanosoma cruzi*, causative agent of Chagas' disease, is reported. The final model at 2.8 Å includes the bound cofactor NAD^+ and 90 water molecules per monomer and resulted in an R_{factor} of 20.1%, R_{free} = 22.3%, with good geometry indicators. The structure has no ions bound at the active site resulting in a large change in the side chain conformation of Arg^{249} which as a consequence forms a salt bridge to Asp^{210} in the present structure. We propose that this conformational change could be important for the reaction mechanism and possibly a common feature of many GAPDH structures. Comparison with the human enzyme indicates that interfering with this salt bridge could be a new approach to specific inhibitor design, as the equivalent to Asp^{210} is a leucine in the mammalian enzymes.

© 1998 Federation of European Biochemical Societies.

Key words: Glyceraldehyde-3-phosphate dehydrogenase; Crystal structure; Catalytic mechanism; Conformational change; *Trypanosoma cruzi*

1. Introduction

Chagas' disease, caused by the protozoan *Trypanosoma cruzi*, is estimated to affect some 16–18 million people, mostly from South and Central America, where 25% of the total population are at risk [1]. About 3 million of the infected people have developed severe complications, characterised by chronic cardiopathy, digestive lesions and neurological disorders, causing 45 000 deaths per year and a loss of approximately 3 million disability-adjusted life years (DALYs). Increasing incidence in urban areas of North America has been reported, as a consequence of the flux of immigration from the south. Control of the insect vector (*Triatoma infestans*) in endemic areas has led to a virtual elimination of transmission by insect bites and as a consequence blood transfusion and congenital transmission are currently the major causes for the spread of the disease. Since the discovery of the disease by the Brazilian sanitary physician Carlos Chagas, in 1909, many attempts at treatment have been made, but no effective drug has so far been found. Besides low efficacy, the drugs currently available, nifurtimox and benzonidazole, have strong side effects [2]. The clear need for the development of new drugs against Chagas' disease has stimulated us to initiate a project aimed at the discovery of highly specific inhibitors that could be used as lead compounds through the structure-based design of molecules that could interfere with specific targets of the trypanosomal metabolism.

In 1977, Opperdoes and Borst discovered that the bloodstream form of parasites of the family Trypanosomatidae possesses a microbody-like organelle, the glycosome, where glycolysis takes place. The bloodstream form of the related parasite *Trypanosoma brucei*, the causative agent of sleeping sickness, has no functional tricarboxylic acid cycle and is highly dependent on glycolysis for ATP production [3]. This great dependence on glycolysis as a source of energy makes the glycolytic enzymes attractive targets for trypanocidal drug design. Indeed, three enzymes of this metabolic pathway in *T. brucei* have had their three-dimensional structures determined, triosephosphate isomerase (TIM) [4], glyceraldehyde-3-phosphate dehydrogenase (GAPDH) [5] and phosphoglycerate kinase (PGK) [6]. One of these proteins, glycosomal GAPDH, shows potential target sites with significant differences compared with the homologous human enzyme, and inhibitors have been designed, synthesised and tested [7,8]. These promising results prompted us to initiate the structural study of the same enzyme from *Trypanosoma cruzi* which is reported here. Glycolysis is also a very important metabolic process in the mammalian stages of this latter trypanosomatid species [9].

The enzyme GAPDH is a homotetramer of molecular mass approximately 156 kDa, whose physico-chemical properties are conserved in most species [10]. GAPDH catalyses the oxidative phosphorylation of glyceraldehyde-3-phosphate (GAP) to 1,3-bisphosphoglycerate (BPG). Although the reaction mechanism has been intensively investigated [11–13], there is no general agreement on the molecular mechanisms involved in the regulation of the binding of the substrate to and the release of the product from the active site.

The 3D structures of GAPDH from several other species have been determined crystallographically, including lobster [14], human [15], *Bacillus stearothermophilus* [16], *T. brucei* [5], *Thermotoga maritima* [17], *Thermus aquaticus* [18], *Escherichia coli* [19] and *Anas* sp. [20]. As a common feature of several of these structures, two sulphate ions were found in each monomer, bound at the catalytic site. These ions where thought to occupy the positions of the two phosphate ions involved in the reaction, respectively the phosphate from the substrate (Ps) and the inorganic phosphate (Pi) which is added to the 1-position of the substrate during the reaction. Recently, the crystal structure of GAPDH from *Leishmania mexicana* was determined, in the presence of phosphate instead of

*Corresponding author. Fax: (55) (16) 2749204.
E-mail: oliva@ifqsc.sc.usp.br

0014-5793/98/$19.00 © 1998 Federation of European Biochemical Societies. All rights reserved.
PII S0014-5793(98)00154-9

sulphate [21]. It was found that the binding site for Ps is essentially the same as that observed for the corresponding sulphate ion in the other structures. In contrast, the Pi site was found to be displaced by 2.9 Å and closer to the catalytic histidine residue, with the authors suggesting that this position is more likely to be the active one. The structure of the apoenzyme (in the absence of both cofactor and anions) from *B. stearothermophilus* [16] and lobster [14], and more recently the structures of the enzymes from *E. coli* and *Thermus aquaticus* (complexed with NAD^+ but in the absence of ions), have led to speculations regarding the molecular mechanism of the reaction pathway.

In this work we present the crystallographic structure of GAPDH from *T. cruzi*. The enzyme was also crystallised in the absence of sulphate or phosphate ions and this fact has led to new insights into the possible role of several residues in the regulation and stabilisation of substrate binding and the release of the reaction product.

2. Materials and methods

2.1. Preparation and purification of T. cruzi GAPDH

Recombinant *T. cruzi* GAPDH (TcGAPDH) was prepared and purified according to a modification of a previously reported procedure [22]. TcGAPDH-overproducing *E. coli* were grown at 37°C in LB medium supplemented with glycerol 1%, malic acid 0.4%, casamino acids 0.1%, ampicillin 100 μg/ml and tetracycline 12.5 μg/ml. When the OD_{600} was 0.8 the expression of *T. cruzi* GAPDH was induced by 0.4 mM IPTG at 20°C overnight. The lower temperature during expression was essential for recovering large quantities of soluble and fully active enzyme. The cells were lysed by sonication and the lysates were centrifuged at $20\,000 \times g$ for 20 min. The supernatant was fractionated by ammonium sulphate precipitation (50% saturated) and the resultant mixture centrifuged at $2000 \times g$ for 20 min. The supernatant was further purified by hydrophobic chromatography on a phenyl-sepharose column in which TcGAPDH was eluted with a decreasing $(NH_4)_2SO_4$ gradient. Eluted fractions containing TcGAPDH were pooled and dialysed against $(NH_4)_2SO_4$-free 25 mM Tris-HCl pH 7.8 buffer. The dialysed sample was subsequently further purified by cation-exchange chromatography on a column of phospho ultrogel in which TcGAPDH was eluted with an increasing KCl gradient. Fractions containing GAPDH activity were pooled and dialysed against 25 mM Tris-HCl pH 7.8 buffer, containing 500 mM ammonium sulphate, 2 mM NAD^+, 1 mM azide, DTT and EDTA and concentrated using an Amicon concentrator to a final concentration of 9 mg/ml. The homogeneity of the enzyme was evaluated by SDS-PAGE.

2.2. Crystallisation of T. cruzi GAPDH

Crystals of *T. cruzi* GAPDH were grown at 4°C by hanging drop vapour diffusion, using a protein solution at 9 mg/ml in the above described dialysis buffer and a reservoir solution of 0.1 M sodium cacodylate pH 6.5, 18% polyethylene glycol 8000 and 0.2 M calcium acetate. The crystals grow to a size of $0.1 \times 0.2 \times 0.2$ nm within 10 days, frequently mixed with salt crystals resulting from the reaction of the ammonium sulphate with calcium acetate. The crystals belong to the space group P1 with unit cell dimensions $a = 88.1$ Å, $b = 124.6$ Å, $c = 85.4$ Å, $\alpha = 101.2°$, $\beta = 112.9°$, $\gamma = 83.6°$. Crystal content analysis indicates two tetramers in the unit cell, resulting in a V_m value of 2.53 $Å^3$/Da, close to the average value for other protein crystals [23].

2.3. Data collection

Diffraction intensities were collected with the crystals cooled to 4°C, using a Rigaku RU-200 generator and an R-AXIS II area detector. The crystals are very fragile and sensitive to variations in temperature and precipitant concentration. Four crystals were used, totalling 89 diffraction images of 2° oscillation. The program PROCESS [24] was used to index the images, integrate the intensities, and scale and merge the data. A total of 73 595 reflections were measured between 15 and 2.8 Å resolution and reduced to 54 184 unique reflections (67.1% completeness). The data set has an R_{sym} of 0.125 on intensities (0.20 in the last resolution shell 2.95–2.8 Å).

2.4. Structure determination and refinement

The structure of *T. cruzi* GAPDH was determined by molecular replacement. The search model used was the *T. brucei* GAPDH crystal structure deposited in the PDB (1GGA), from which the NAD^+ cofactor, sulphate ions and water molecules were removed. The overall sequence identity between TcGAPDH and TbGAPDH is 90% [22]. The program AMoRe [25] was used for the rotation and translation functions using the data from 15 to 3.5 Å resolution. Two solutions for the rotation matrix were determined which are associated with the two *T. cruzi* GAPDH tetramers in the primitive cell. With one of the tetramers centred at the origin, the translation function for the second tetramer presented a unique solution with a correlation coefficient of 58.4%, a value double that of the second highest peak. This solution resulted in a crystalline packing which presented no steric hindrance, good intermolecular contacts and a compatible solvent content.

The refinement of the structure was performed using the X-PLOR program [26] including data in the range 8.0–2.8 Å. The search model after rotation and translation, was submitted to rigid body refinement, considering the eight subunits as independent rigid structures. From this point onwards, strict non-crystallographic symmetry was imposed. After determining the matrix and vectors which superimpose one independent subunit to the other seven, a molecular mask for one of the subunits was constructed using the program MAMA [27]. Electron density maps $w(2F_o - F_c)$ for the eight subunits were calculated using the package of programs CCP4 [28]. The 8-fold averaged map was then calculated starting from the molecular envelope and the individual electron density maps using the RAVE package [29]. The averaged map analysis allowed the unambiguous fitting of the correct *T. cruzi* residues into the initial *T. brucei* GAPDH model, using the program O [30].

After this procedure, a new cycle of rigid body refinement was conducted leading to an R_{factor} of 0.328. The non-crystallographic symmetry (NCS) operations were recalculated and strictly imposed throughout the subsequent model refinement. The 8-fold NCS ensures an excellent ratio of refined parameters per observation, despite the relatively low completeness of the dataset. The use of strict NCS constraints in the refinement of protein structures has been strongly recommended [31], to reflect the widely observed fact that identical sequences correspond to identical structures. To carefully scrutinise this assumption in the present study, in all steps of the refinement both averaged and non-averaged electron density maps for all eight molecules in the unit cell were simultaneously displayed in order to identify possible regions of discrepancies, nothing being found to justify any independent refinement.

Six refinement cycles of simulated annealing with temperatures ranging from 3000 K to 300 K with 50 K steps, followed by positional refinement, group B-factor refinement and finally individual B-factors refinement were performed. At this stage the NAD^+ cofactor could be built into the remaining electron density. Some water molecules were also assigned from difference Fourier maps, located with the program PICKWATER from CCP4 [28]. Unlike the *T. brucei* crystal structure, no sulphate or phosphate ions were found at the active site. Therefore, the final model of the refined glycosomal TcGAPDH monomer has 359 residues, 1 NAD^+ molecule and 90 water molecules. Some of the C-terminal residues did not show electron density for the side chains and were refined with zero occupancies for all side chain atoms beyond Cβ. The final R_{factor} was 0.201 and the R_{free} 0.223 (10% of reflections were used in the calculation of R_{free}). This comparatively low value of the R_{free} can be correlated to the 8-fold NCS used throughout the refinement, although still an indicator of the unbiasing of the refinement [29]. Atomic co-ordinates have been submitted for deposition at the Brookhaven data base.

3. Results and discussion

3.1. Quality of the structure

The use of 8-fold strict NCS throughout the structure refinement has contributed to produce very good electron density for the available resolution, with the exception of the loop comprising residues 66–76 and some residues at the N- and C-termini. An example of the quality of the electron density is presented in Fig. 1.

The rms deviations from ideality for the final structure are

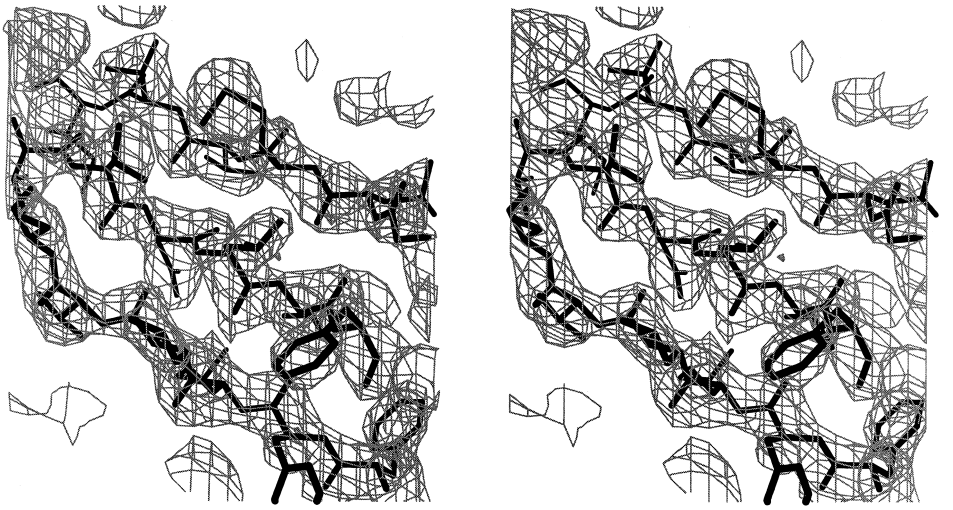

Fig. 1. Stereo view of a slab of the final ($2F_o-F_c$) electron density map contoured at a level of 3σ showing a region of β sheet centred on Leu[260]. Figure produced using the graphics program O [30].

0.009 Å in bond lengths, 1.639° for bond angles and 25.20° for dihedral angles. The average temperature factor values for the main chain and side chain atoms of the 359 residues are 22.9 Å^2 and 27.0 Å^2, respectively. The torsion angles for 99.7% of the residues are in the favourable regions in the Ramachandran diagram [32]. Val[255] is the only residue found in a unfavourable region, with torsion angles of $\phi = 87°$ and $\varphi = 125°$. This residue is located in a loop between two consecutive β strands. The unfavourable conformation of this residue is conserved in all other GAPDH structures available, and is probably maintained in order to contribute to the correct positioning of the active residue Cys[166] and the nicotinamide ring of the NAD$^+$ cofactor. As shown in Fig. 2, the side chain of Cys[166] is in Van der Waals contact with the Cβ of Asn[335], whose side chain oxygen forms a hydrogen bond with the main chain nitrogen of Val[255]. This hydrogen bond stabilises the asparagine rotamer such that its side chain nitrogen is in the correct orientation to donate a second hydrogen bond to the amide of the incoming NAD$^+$ during catalysis.

3.2. Description of the structure

The Tc-GAPDH tetramer has four subunits arranged with local 222 symmetry. Each subunit is composed of two domains: the N-terminal or NAD$^+$ binding domain and the C-terminal or catalytic domain. The N-terminal domain contains approximately 150 residues comprised of two typical Rossmann folds forming a 6-stranded parallel β-sheet surrounded by α-helices on both sides. This domain contains the loop formed by residues 66–76, found only in the GAPDH of the Trypanosomatidae family (*T. cruzi*, *T. brucei*, *L. mex-*

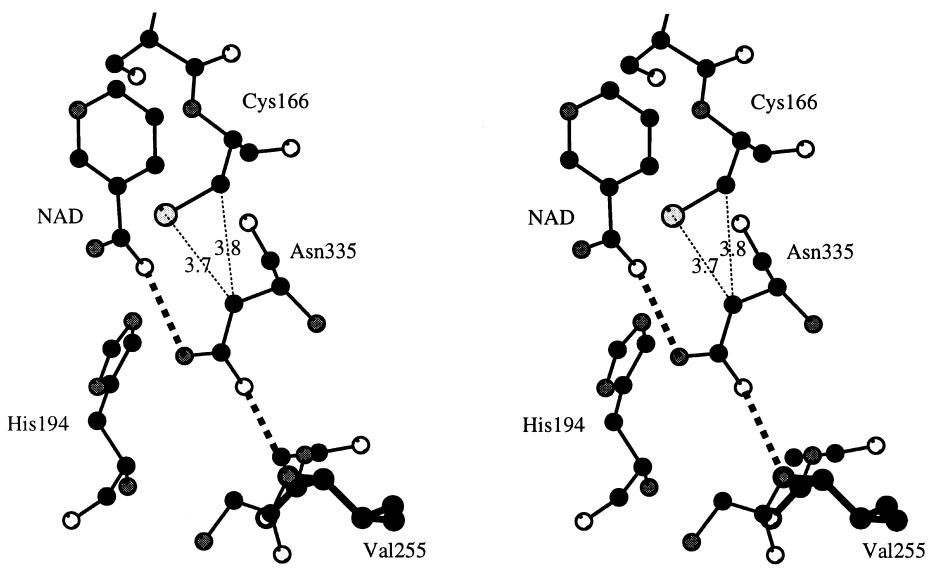

Fig. 2. Stereo view of the active site showing the side chain of the catalytic cysteine (Cys[166]) in Van der Waals contact with Asn[335], whose side chain amide forms hydrogen bonds simultaneously with the main chain nitrogen of Val[255] and the nicotinamide ring of the NAD$^+$ cofactor. Val[255] adopts a disallowed main chain conformation which is observed in all other GAPDH structures and probably related to the need to orientate correctly the side chain of Asn[335] in order to receive the incoming cofactor. The figure was produced using the program MOLSCRIPT [33].

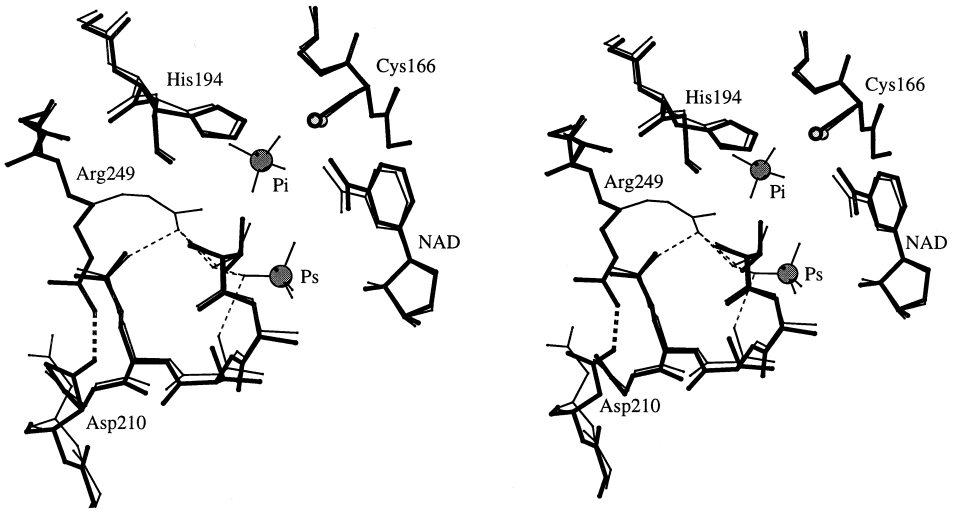

Fig. 3. Stereo view of the active site of *T. cruzi* GAPDH (in bold) superimposed on that of *B. stearothermophilus,* showing the large difference in the Arg^{249} side chain conformation. The sulphate ions encountered in the *B. stearothermophilus* structure which correspond to the substrate and inorganic phosphate binding sites are indicated as Ps and Pi respectively. In *T. cruzi*, in the absence of anions, Arg^{249} has swung out of the active site and forms a salt bridge to Asp^{210} whilst in *B. stearothermophilus* it points towards the substrate phosphate forming hydrogen bonds with Thr^{197} and Gln^{200}. The figure was produced using MOLSCRIPT [33].

icana). The catalytic domain is of the α/β class and includes the essential residues for the catalytic activity, Cys^{166} and His^{194}.

The structures of GAPDH from *T. cruzi* and *T. brucei* are very similar, as expected from their high sequence identity (90%). The superposition of the two structures has an rms deviation of 0.53 Å, for all Cαs. Some differences occur at the N- and C-terminal regions, which were partially disordered in the *T. brucei* structure, and could be better interpreted in the current study.

3.3. NAD^+ binding site

The binding site of the adenosine ring of the NAD^+ cofactor has been studied in *T. brucei* GAPDH and explored as a good target for rational drug design [7], mainly because of important differences between the parasite and the homologous human enzyme.

In the cofactor binding site, two regions could be explored for specific inhibitor design. In one of them, the presence of residues Leu^{113} and Gln^{91} in *T. brucei* GAPDH, results in differences in polarity and volume when compared with the corresponding residues in the human enzyme. Compounds have been designed based on adenosine derivatives that aim to exploit these differences [7]. We find that in this region *T. cruzi* GAPDH is structurally conserved with respect to the related *T. brucei* enzyme and therefore could also be a good target site for the design of specific inhibitors for Chagas' disease.

The other region that was identified as a good target is the interface between two neighbouring subunits of the active tetramer and also close to the binding site of the adenosine moiety of the NAD^+ cofactor. In this region, a hydrophobic pocket of approximately 10 Å width is formed in the trypanosomal enzyme which is essentially absent in the human enzyme, due to a difference in the course of the main chain caused by the presence of Pro^{190}. The residues that participate in this pocket are Met^{38}, Val^{205} and Asp^{39} in *T. cruzi*, which are replaced by Phe^{36}, Pro^{190} and Ile^{37} in the human enzyme.

Compounds that could still fit the NAD^+ binding site but which possess bulkier substituents capable of exploiting the adjacent hydrophobic pocket in the parasite enzyme would possibly have little affinity for human GAPDH, leading to potential specific inhibitors. With this strategy, adenosine derivatives were designed, synthesised and kinetically characterised with respect to the enzymes from *T. brucei* and *L. mexicana* [7], showing good affinity and selectivity when compared with the human enzyme.

In the *T. cruzi* enzyme, the hydrophobic pocket is slightly more closed than in the *T. brucei* structure, being only 9 Å wide. This could be a consequence of the absence of ions bound to the active site, as discussed in the following section, which might hinder the binding of compounds designed based on the *T. brucei* structure. The *T. cruzi* structure, in fact, should represent the in vivo condition in which the inhibitor would normally encounter the target enzyme, i.e. with neither substrate nor inorganic phosphate bound.

3.4. The catalytic site

The catalytic site is composed of the region involving the nicotinamide moiety of the NAD+ cofactor and the residues that participate in catalysis. This region has not yet been exploit for structure-based drug design, mainly because it shows high sequence and structural conservation as a consequence of the selective pressure for activity.

A singular feature of the present structure is the fact that the enzyme has been crystallised in the absence of phosphate or sulphate ions and therefore with an empty active site. No ordered water molecules were identified within the active site pocket. As a consequence, Arg^{249}, essential for the stabilisation of charges around the Ps binding site, has shown a large conformational change. When compared with the structure of *B. stearothermophilus* (1.8 Å resolution), this transition results in a total displacement of 5.2 Å in the position of the Cξ atom of the guanidinium moiety, which is then in position to form a salt bridge to residue Asp^{210}. This has pointed to a possibly important gating mechanism to regulate the binding of the substrate to the active site and the release of the product after the completion of the reaction. Indeed, analysis of several

other GAPDHs with known 3D structures have shown the conservation of this aspartic acid residue, in position to form a salt bridge to the arginine residue. In the active site of the structures of the human and duck enzymes, not only the Asp residue has been substituted by Leu, but a complementary substitution is also observed, i.e. Gly^{213} in *T. cruzi* is replaced by Asp. As a result, the mammalian and avian enzyme structures show the carboxylate of the Asp side chain to approach approximately the same position as Asp^{210} in *T. cruzi*. This is suggestive that Asp^{197} in human GAPDH (the homologue of Gly^{213} in *T. cruzi*) may play a similar role to that of Asp^{210} in the parasite enzyme in stabilising the arginine in the absence of substrate. Fig. 3 compares the structures of *T. cruzi* and *L. mexicana* in this region highlighting the conformational change of Arg^{249}. Two recently published structures of GAPDH, from *E. coli* and *T. aquaticus*, were also crystallised without anions bound to the active site. In the case of *E. coli*, Arg^{231} (equivalent to Arg^{249} in *T. cruzi*) was found to be in two alternate positions in one of the monomers in the asymmetric unit and in the salt-bridged conformation in the other. These data indicate the high flexibility of the side chain of this residue, reinforcing that its movement could be important in the regulation of the attachment of the substrate and the release of the reaction product. The *T. aquaticus* structure has the side chain of Arg^{231} in each of the four monomers of the asymmetric unit in the closed conformation, that is, at the position of co-ordination to the substrate phosphate despite the absence of anions. All the thermostable structures have a special feature in this respect, as they all show an extra arginine residue at the active site, also in position to co-ordinate Ps, as in *B. stearothermophilus*. This second Arg residue (Arg^{195} in *B. stearothermophilus*) hinders the movement of the side chain of Arg^{231} (equivalent to Arg^{249} in *T. cruzi*) to form the salt bridge with Asp^{192}, thus impeding the gating mechanism described above. It is thus possible that in thermophilic bacteria the Ps binding site is preformed prior to substrate binding.

3.5. Implications for drug design

These new findings related to the active site suggest a potential new target for selective inhibition. The substitution of Asp^{210} (*T. cruzi*) by Leu^{194} (human) suggests that compounds that partially occupy the active site and at the same time make polar interactions with the Asp^{210} side chain could show increased specificity for the parasitic enzyme. Alternatively, in view of the proposed physiologically important gating mechanism involving the active site Arg^{249}, any compound that could specifically interact with Asp^{210} and therefore interfere with the salt bridge formed with Arg^{249}, would be a potential specific inhibitor. Prospective compounds are being designed and synthesised to evaluate these possibilities.

Acknowledgements: G.O. is a Howard Hughes Medical Institute International Scholar. We thank the Fundação de Amparo à Pesquisa do Estado de São Paulo (Grant 94/0587-9), Programa de Apoio ao Desenvolvimento Científico e Tecnológico/SBIO (Grant 62.0137/95.9) and the World Health Organisation (TDR Grant 940854), and the European Commission (INCO-DC Programme) for financial support. B.G.G. is supported by a grant from the Brazilian National Research Council and D.H.F.S. has a post-graduate fellowship from FAPESP. We thank Prof. F. Opperdoes for his kind encouragement and support throughout this project.

References

[1] World Health Organisation Statistical Information System Website, at http://www.who.ch./whosis/whosis.htm
[2] Kirchhoff, L.V. (1993) New Engl. J. Med. 329, 639–644.
[3] Opperdoes, F.R. (1987) Annu. Rev. Microbiol. 41, 127–151.
[4] Wierenga, R.K., Noble, M.E.M., Vriend, G., Nauche, S. and Hol, W.G.J. (1991) J. Mol. Biol. 220, 995–1015.
[5] Vellieux, F.M.D., Hajdu, J., Verlinde, C.L.M.J., Groendijk, H., Read, R.J., Greenhough, T.J., Campbell, J.W., Kalk, K.H., Littlechild, J.A., Watson, H.C. and Hol, W.G.J. (1993) Proc. Natl. Acad. Sci. USA 20, 2355–2359.
[6] Bernstein, B.E., Michels, P.A.M. and Hol, W.G.J. (1997) Nature 385, 275–278.
[7] Verlinde, C.L.M., Callens, M., Van Calenbergh, S., Van Aerschot, A., Herdewijn, P., Hannaert, V., Michels, P.A.M., Opperdoes, F.R. and Hol, W.G.J. (1994) J. Med. Chem. 37, 3605–3613.
[8] Verlinde, C.L.M.J., Merrit, T.E.A., Van Den Akker, F., Kim, H., Feil, I., Delboni, L.F., Mamde, S.C., Sarfaty, S., Petra, P.H. and Hol, W.G.J. (1994) Protein Sci. 3, 1670–1686.
[9] Engel, J.C., Franke de Cazzulo, B.M., Stoppani, A.O., Cannatta, J.J. and Cazzullo, J.J. (1987) Mol. Biochem. Parasitol. 26, 1–10.
[10] Seydoux, F., Bernhard, S., Pfenninger, O., Payne, M. and Malhota, O.P. (1973) Biochemistry 12, 4290–4300.
[11] Duggleby, R.G. and Dennis, D.T. (1974) J. Biol. Chem. 249, 167–174.
[12] Harrigan, P.J. and Trentham, D.R. (1973) Biochem. J. 135, 695–703.
[13] Segal, H.L. and Boyer, P.D. (1953) J. Biol. Chem. 204, 265–281.
[14] Moras, D., Olsen, K.W., Sabesan, M.N., Buehner, M., Ford, G.C. and Rossmann, M.G. (1975) J. Biol. Chem. 250, 9137–9162.
[15] Watson, H.C., Duee, E. and Mercer, W.D. (1972) Nature New Biol. 240, 130.
[16] Skarzynski, T., Moody, P.C.E. and Wonacott, A.J. (1987) J. Mol. Biol. 193, 171–187.
[17] Korndörfer, I., Steipe, B., Huber, R., Tornschy, A. and Jaenicke, R. (1995) J. Mol. Biol. 246, 511–521.
[18] Tanner, J., Hecht, R.M., Pisegna, M., Seth, D.M. and Krause, K.L. (1994) Acta Crystallogr. D50, 744–748; PDB access code 1CER.
[19] Duée, E., Olivier-Deyris, L., Fanchon, E., Corbier, C., Branlant, G. and Dideberg, O. (1996) J. Mol. Biol. 257, 814–838.
[20] Barbosa, V.M. (1996) PhD Thesis, University of São Paulo.
[21] Kim, H., Feil, I.K., Verlinde, C.L.M., Petra, P.H. and Hol, W.G.J. (1995) Biochemistry 34, 14975–14986.
[22] Hannaert, V., Opperdoes, F.R. and Michels, P.A.M. (1995) Protein Express. Purif. 6, 244–250.
[23] Matheus, B.W. (1968) J. Mol. Biol. 33, 491–497.
[24] Process Program, Instruction Manual of R-AXIS IIC.
[25] Navaza, J. (1994) Acta Crystallogr. A50, 157–163.
[26] Brunger, A.T. (1992) X-PLOR, A System for X-ray Crystallography and NMR, Version 3.1, Yale University Press, New Haven, CT.
[27] Kleywegt, G.J. and Jones, T.A. (1994) Manual do programa MAMA, University of Uppsala.
[28] CCP4 Program Suite Rotation Function-ALMN (1994) User Documentation, Daresbury Laboratory.
[29] Kleywegt, G.J. and Jones, T.A. (1994) RAVE, The Manual, Uppsala.
[30] Jones, T.A. and Kjeldgaard, M. (1993) 'O', The Manual, Version 5.9, Uppsala.
[31] Kleywegt, G.J. and Jones, T.A. (1995) Structure 3, 535–540.
[32] Laskowski, R.A., MacArthur, M.W. and Thornton, J.M. (1993) J. Appl. Crystallogr. 26, 283–291.
[33] Kraulis, P.J. (1991) J. Appl. Crystallogr. 24, 946–950.